WELDING RESEARCH

SUPPLEMENT TO THE *WELDING JOURNAL*, September 2004
Sponsored by the American Welding Society and the Welding Research Council

Reliability of Weld Microstructure and Property Calculations

The AWS 2004 Adams Lecture explores modeling vs. experimentation for developing welding consumables for new alloys

BY H. K. D. H. BHADESHIA

We depend in our everyday life on the performance of vast quantities of steel, which we use without giving it a second thought. This is possible because the material is reliable and cheap (weight for weight, some 1000 times cheaper than potato chips). Yet, there are remarkable technologies and sciences working behind the scenes to create ever better steels that can be assembled into awe inspiring structures.

Examples include the giant oil rigs that pepper the North Sea, the oil and gas pipelines that traverse the frozen wastes, and the 101 Tower in Taiwan, which is now the tallest building in the world — Fig. 1. These are all made from steel and rely on welding for their assembly.

Weld Design: Experiment or Model?

A weld is a heterogeneity introduced into a carefully manufactured steel. It is a defect that has to be managed. One way of doing this is through a deep understanding of metallurgy, thereby avoiding the engineering disasters of the kind that plagued for example, the Liberty ships. A weld consists of distinct zones, each of which is the consequence of a particular interaction between heat flow and the phase transformation characteristics of the weld metal and the base metal.

Out of all these zones, the weld metal is particularly challenging to design because there is little that can be done once the weld is completed (Refs. 1–3). This contrasts with wrought steel, which can be processed and manicured using all the facilities available in a modern steel plant. There is, therefore, a major industry devoted to the design and manufacture of welding alloys. Academic activity has supported this industry, both in terms of the underlying science and in the creation of quantitative methods for alloy design. Given all this effort, I shall use this lecture to explore whether it is any longer necessary to conduct experiments when developing welding consumables. Are the models sufficiently robust to be exploited by industry without supervision?

The focus of this paper is on ferritic steels, which form the bulk of the billion or so tons of steel consumed annually. The development of welding consumables involves all weld-metal tests in which a joint is deposited such that samples can be obtained without dilution with the base plates. It is fortunate that the literature is rich in data from tests of this kind, data which have been liberally exploited in the development of models.

HARSHAD K. D. H. BHADESHIA was selected to present the 2004 Comfort A. Adams lecture at the AWS Annual Meeting, Chicago, Ill. He is a professor of physical metallurgy in the Department of Materials Science and Metallurgy at the University of Cambridge, U.K., where he received his Ph.D. He has held the positions of university demonstrator, university lecturer, reader in physical metallurgy, and Royal Society Leverhume Trust Senior Fellow.

He specializes in the theory of solid-state transformations with emphasis on the prediction of microstructural development in complex metallic alloys, particularly for multicomponent steels as applied to engineering applications.

He was elected a Fellow of the Royal Society, the Institute of Physics, the Institute of Materials, and the Royal Academy of Engineering, and this year was awarded Consulting Professorship by Harbin Institute of Technology, China. He has received other honors from institutions in Brazil, Japan, India, and the United States. He can be contacted at www.msm.cam.ac.uk/phase-trans.

KEY WORDS

Consumables
Cooling Curve
Experimentation
Ferritic Steel
Modeling
Solid-State Transformation

Defining Characteristics of a Weld Metal

The essential variables needed in order to be able to calculate the microstructure and properties of steel weld metal are illustrated in the top row of Fig. 2 (Refs. 4, 5). The chemical composition, cooling conditions, and austenite grain size capture all the essential features of weld metal. The essence of the welding process and joint geometry is expressed via the cooling curve and there are many models with varying levels of sophistication capable of predicting the change in temperature as a function of time and position. As will be seen later, the chemical composition defines the thermodynamics of transformation and the nature of the heterogeneities that arise.

The austenite grain structure, a parameter sometimes ignored in the interpretation of microstructures, has a profound effect.

Cooling Curve

There is a huge amount of research that has been devoted solely to the calculation of the thermal cycle associated with welding. The most sophisticated of models account for joint geometry, gravitational forces, surface tension effects, buoyancy forces, electromagnetic forces, metal transfer, changes in thermophysical properties with temperature and turbulence, etc. (Ref. 6). Weld pool shapes can be fairly accurately calculated and when there are deviations, empirical correc-

Fig. 1 — The 101 Tower in Taiwan, made from steel and glass. Photograph courtesy of Thomas Sourmail.

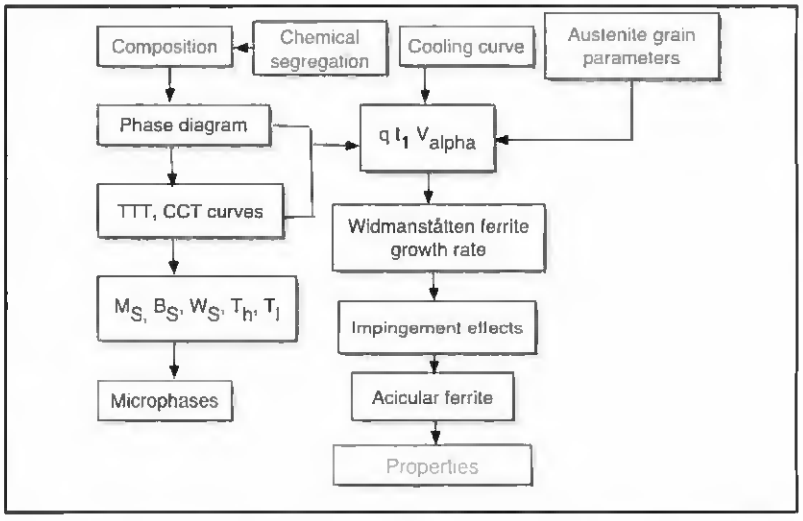

Fig. 2 — Flowchart showing the progress of weld metal microstructure and property calculations.

tions are made in a manner constrained by the physics. From the present point of view, it is really the cooling curve that is important, particularly in the regime where solid-state transformations occur, i.e., between about 900°C and the martensite-start temperature; this must be the reason why the time $\Delta t_{800-500}$ is a popular measure in the welding industry. This greatly simplifies the problem because the cooling rate (dT/dt) within the weld metal can, to a high level of accuracy, be represented independently of position with a simple equation (Refs. 7, 8).

$$\frac{dT}{dt} = \frac{C_1 (T - T_i)^{C_2}}{Q\eta} \qquad (1)$$

where Q is the heat input per unit length, η is the transfer efficiency, and T_i the preheat or interpass temperature. There are numerous weld cooling curves available in the welding literature; for a particular process and weld geometry, this equation can be fitted to derive the empirical constants C_1 and C_2. Such constants are available for a large variety of welding processes and this simple procedure works rather well in practice. Rigorous calculations in which the weld pool is properly modeled make only a small difference to the calculated microstructure. This is because the cooling rate in the transformation range is relatively insensitive to fluid flow phenomena.

The Austenite Grain Structure

The columnar austenite grains in the weld deposit derive, in most cases, from columnar δ-ferrite grains that grow epitaxially from the fusion surface during the early stages of solidification. The columnar shape is quite different from the equiaxed grains found in most steels and requires a different approach in defining the amount of austenite grain surface per unit volume (S_V). It has been demonstrated that the columnar grains can be described as hexagonal prisms (length c and side a) in three dimensions. It follows that two stereological parameters, the mean lineal and mean areal intercepts, are needed to quantify this anisotropic grain structure. However, because the grains are much longer than they are wide, a good approximation is that the mean lineal intercept measured on transverse sections of the weld (L_m), in a direction normal to the columns, adequately describes S_V (Ref. 9). There exist equations that then relate S_V to the chemical composition of the weld metal and the heat input.

The Alloying Elements

A weld metal may contain twenty or more deliberate solutes, and others that are introduced accidentally during deposition: C, Mn, Si, Ni, Mo, Cr, V, Co, B, N, O ..... Some of these, such as boron, may be present in minute quantities and yet can have a profound effect on the microstructure. Solutes act on steels by two essential mechanisms:

1) The relative stabilities of austenite (γ) and ferrite (α) are affected via a thermodynamic effect, which can be expressed rigorously in terms of the difference in Gibbs free energies, $G^\alpha - G^\gamma$, often called the "driving force" for transformation. This thermodynamic quantity feeds directly into rate theory, for example in the equations governing classical nucleation. It is now routinely possible to calculate these free energies and, of course, to express them in terms of equilibrium phase diagrams. Such calculations can now be conducted routinely for multicomponent, multiphase steels, using proprietary or free software.

2) The second effect is more subtle because it depends on the rate at which change occurs. The equilibrium solubility of an alloying element is never identical in austenite and ferrite. If circumstances permit, the solute will therefore tend to partition between the phases during the course of transformation. The required diffusion may then limit the kinetics of the process. This is a gross effect involving large numbers of atoms and distances comparable to the size of the transformed product. Another kinetic effect of equal importance can be triggered by minute concentrations of solute; misfitting atoms can segregate to interfaces. In doing so, they reduce the interfacial energy per unit area. This is the mechanism by which boron renders austenite grain boundaries less effective as heterogeneous nucleation sites for ferrite. Traces of boron can therefore have a huge influence on hardenability, far in excess of that expected from its influence on $G^\alpha - G^\gamma$.

Solid-State Transformations

Allotriomorphic Ferrite

Having described the three parameters that are seminal in the development of weld metal microstructure, we now address the complex array of phase changes that occur as the weld metal cools (Refs. 1–5). The essential features of the transformed microstructure are illustrated schematically in Fig. 3. It consists of allotriomorphic ferrite α, Widmanstätten ferrite α_w, acicular ferrite α, and the so-called microphases, which might include small amounts of martensite, retained austenite, or degenerate pearlite. Bainite consisting of sheaves of parallel platelets is also found in some weld de-

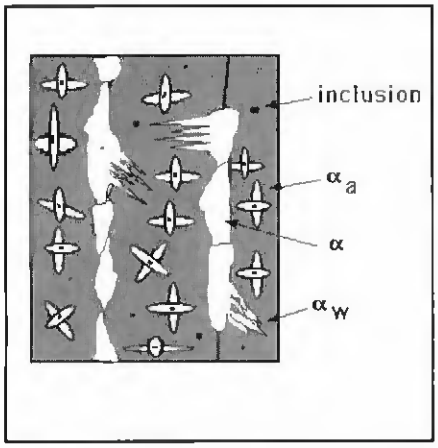

Fig. 3 — Schematic representation of the microstructure of weld metal.

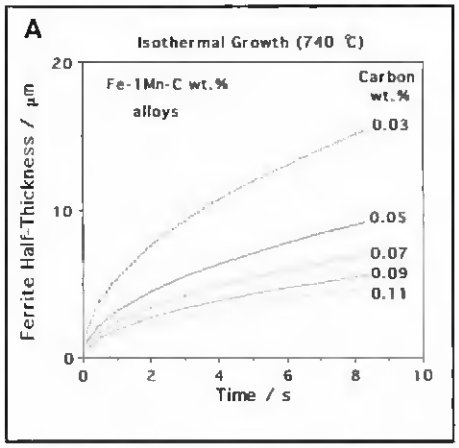

Fig. 4 — A — Isothermal thickening of ferrite layers as a function of the carbon concentration; B — correlation of parabolic rate constant against v_a for a variety of welds.

posits, particularly of the type used in the power generation industry.

These phases all evolve during cooling, beginning with the decoration of austenite grain boundaries with layers of allotriomorphic ferrite. They seem to nucleate readily and then thicken at a rate controlled by the diffusion of carbon in the austenite (γ) ahead of the α/γ interface. The substitutional elements do not partition; this kind of transformation is said to occur under paraequilibrium conditions. Theory shows that the thickness (q) of the ferrite varies parabolically with time (t)

$$q = \alpha_1 t^{1/2} \tag{2}$$

where α_1, the parabolic thickening rate constant, is given by the solution of

$$2\sqrt{\frac{\underline{D}}{\pi}}\frac{x^{\gamma\alpha}-\bar{x}}{x^{\gamma\alpha}-x^{\alpha\gamma}} = \alpha_1 \exp\left\{\frac{\alpha_1^2}{4\underline{D}}\right\}\operatorname{erfc}\left\{\frac{\alpha_1}{2\sqrt{\underline{D}}}\right\} \tag{3}$$

and $x^{\gamma\alpha}$ $x^{\alpha\gamma}$ are the paraequilibrium carbon concentrations in austenite and ferrite respectively at the interface (obtained using the thermodynamic calculations described earlier), $\bar{x}$ is the average carbon concentration in the alloy and $\underline{D}$ is a weighted average diffusivity of carbon in austenite, given by

$$\underline{D} = \int_{x^{\gamma\alpha}}^{\bar{x}} \frac{D\{x\}dx}{\bar{x}-x^{\gamma\alpha}} \tag{4}$$

where D is the diffusivity of carbon in austenite at a particular concentration of carbon. Some example calculations are illustrated in Fig. 4A, which shows that the thickness is most sensitive to the carbon concentration when the latter is close to the solubility of carbon in ferrite; this is because the need to partition carbon decreases as the average concentration $\bar{x} \rightarrow x^{\alpha\gamma}$. We shall see later that this explains some of the carbon equivalent equations prevalent in industry. Figure 4B shows that the the nucleation stage of the layers of ferrite can justifiably be neglected because the volume fraction v_α correlates strongly with α_1 for a large variety of weld metals.

Welds cool continuously, so the above equations need to be integrated over the temperature range T_h to T_l, the start and stop temperatures for α. T_h is estimated using calculated time-temperature-transformation (TTT) diagrams (Ref. 10) (Fig. 5) and Scheil's rule. T_l is taken to be the point where displacive transformations become kinetically favored. Once the thickness of the layers of α has been calculated, it is straightforward to relate it to the volume fraction of ferrite using the geometry of the austenite grains

$$v_\alpha = \left[\frac{2q\ \tan\{30deg\}}{\left(2a - 2q\ \tan\{30deg\}\right)}\right]/a^2 \tag{5}$$

so that the dependence on austenite grain size becomes obvious.

Widmanstätten Ferrite

Widmanstätten ferrite plates grow with paraequilibrium and lengthen at a rate (G) controlled by the diffusion of carbon ahead of the plate tips. Because of the displacements associated with the transformation, it is necessary to account for strain energy. The plates are confined within the austenite grains in which they nucleate, and they grow so fast that crossing the grains within a fraction of a second is typical — Fig. 6A. The theory used here is rigorous and proven, but the volume fraction of Widmanstätten ferrite (v_W) hardly correlates with G — Fig. 6B.

The discrepancy arises because by the time the weld has cooled to induce Widmanstätten ferrite, acicular ferrite sprouts from inclusions dispersed within the austenite grains. There is, therefore, competition for the austenite that remains and a strong possibility of impingement between intragranularly nucleated acicular ferrite and Widmanstätten ferrite. As illustrated in Fig. 7, when the alloy content is small, the rapid growth of α and α_W consumes much of the austenite, thereby reducing the ability to form α_a. By contrast, in high-hardenability welding alloys, the acicular ferrite has an opportunity to develop and indeed to stifle the penetration of Widmanstätten ferrite into the austenite grains.

The volume fraction of Widmanstätten ferrite that can form is therefore a function not just of the growth rate, but also of the thickness of allotriomorphic ferrite, the time required for it to grow across an austenite grain, and the geometry of the austenite grains.

$$v_W = C_4 G(2a - 4q\ \tan\{30deg\}t_2^2/\left(2a\right)^2 \tag{6}$$

where C_4 is a constant independent of alloy composition and t_2 is a function of the impingement process. As will be seen later, with this accounting, good agreement is obtained with experiments.

Finally, it is worth saying something about acicular ferrite, which is a highly desirable phase (Refs. 1–5). Its microstructure consists of intragranularly nucleated

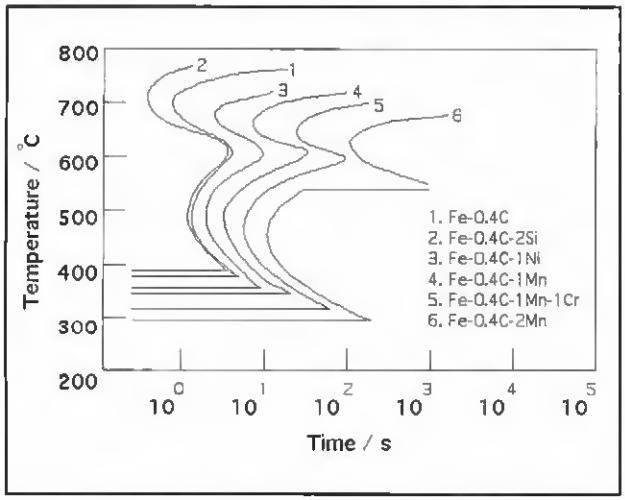

Fig. 5 — Calculated TTT diagrams for a variety of alloys. Each diagram consists of two C-curves, the higher temperature one representing reconstructive reactions (e.g. α) and the lower curve, displacive transformations (α_W, α_a, α_b).

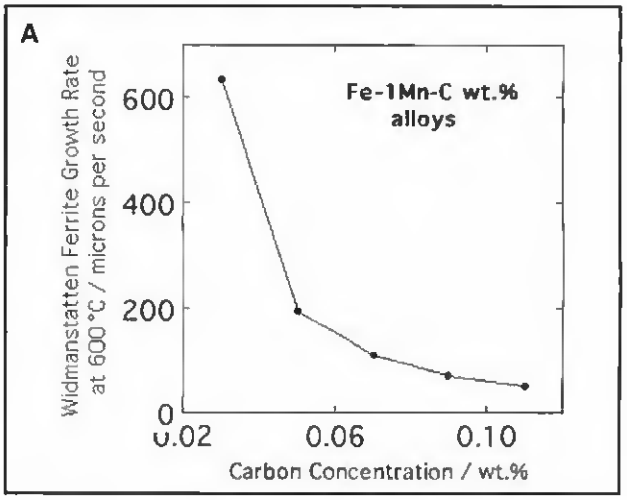

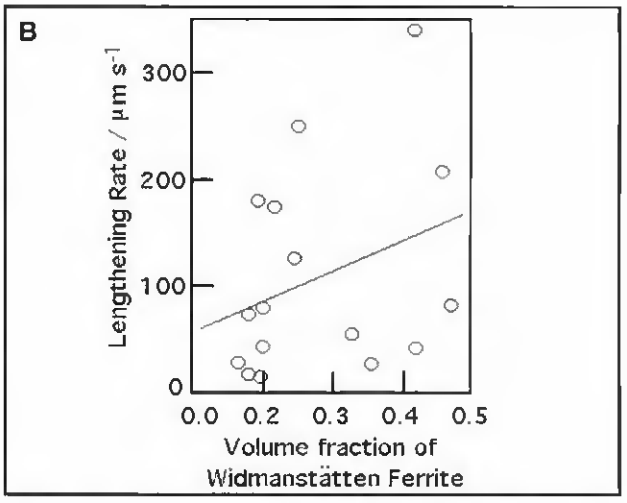

Fig. 6 — A — Calculated growth rate of α_W; B — poor correlation between volume fraction and growth rate of Widmanstätten ferrite.

plates, which radiate in many directions from point nucleation sites. This leads to a chaotic microstructure, which is good at deflecting cracks. It is therefore strong and tough. There is much evidence to suggest that acicular ferrite is intragranularly nucleated bainite, the heterogeneous nucleation sites being the complex nonmetallic inclusions common in welds, either as impurities or as deliberate additions. There is considerable qualitative understanding on the type of inclusions that are most favorable.

There also exist quantitative methods of estimating the type of inclusion that will form during solidification and subsequent cooling. The quantitative details of the calculation of acicular ferrite are discussed elsewhere (Ref. 11).

Solidification-Induced Segregation

In the discussion above, it has been assumed that the chemical composition of weld metal is uniform. This is not the case in practice because welds cool rapidly and there may be uncontrolled variations in the welding conditions. A good estimate of the magnitude of segregation comes from the partition coefficient k_i, which is the ratio of solute concentration i in the solid to that in the liquid. The coefficient can easily be calculated, and used to give the compositions of the solute-rich and solute-poor regions of the weld (carbon is very mobile so it is assumed to be uniformly distributed). This information can then be used to estimate the effect on T_h for allotriomorphic ferrite, which then influences all subsequent transformations.

To summarize, virtually every component of weld microstructure is amenable to calculation. Some examples are presented in Fig. 8. Predictions like these have been extensively validated using published experimental data and by designing new experiments.

An interesting prediction to emerge from these calculations is that the microstructure is sensitive to the carbon when its concentration is comparable to its solubility in ferrite. It seems that the welding industry has implicitly recognized this by proposing two different equations for the carbon equivalent.

$$\text{IIW} \quad > 0.18\ \text{wt-\%}\ \text{C}$$

$$\text{CE} = \text{C} + \frac{\text{Mn}+\text{Si}}{6} + \frac{\text{Ni}+\text{Cu}}{15} + \frac{\text{Cr}+\text{Mo}+\text{V}}{5}\ \text{wt-\%} \qquad (7)$$

$$\text{Ito-Bessyo} \quad < 0.18\ \text{wt-\%}\ \text{C}$$

$$\text{CE} = \text{C} + \frac{\text{Si}}{30} + \frac{\text{Mn}+\text{Cu}+\text{Cr}}{20} + \frac{\text{Ni}}{60} + \frac{\text{Mo}}{15} + \frac{\text{V}}{10} + 5\text{B}\ \text{wt-\%} \qquad (8)$$

For the IIW version, the dependence of CE on substitutional solutes such as manganese is greater than for the CE reserved for low-carbon steels. This is because in the low-carbon steels, it is the carbon that has a greater influence on the kinetics of transformation.

Yield Strength

For an individual phase, the strength can be factorized into a number of intrinsic components (Ref. 12).

$$\sigma = \sigma_{Fe} + \sum_i x_i \sigma_{SSi} + x_C \sigma_C + K_L\{L\} + K_D \rho_D^{0.5} \qquad (9)$$

where x_i is the concentration of a substitutional solute which is represented here by a subscript i. The other terms in this equation can be listed as follows:

K_L strengthening due to grain size, 115 MN m^{-1}.

K_D dislocation strengthening, 7.34×10^{-6} MN m^{-1}

σ_{Fe} pure, annealed Fe, 219 MN m^{-2} at 300 K

σ_{SSi} substitutional solute (i) strengthening

σ_C solid solution strengthening due to carbon

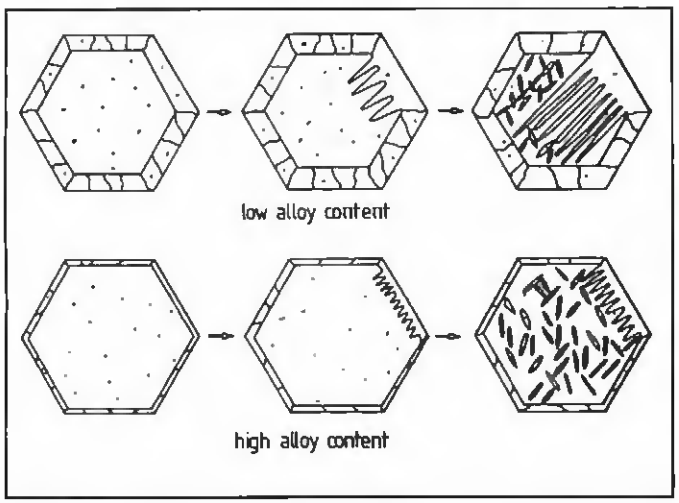

Fig. 7 — The hexagons are cross sections of columnar austenite grains and the dots represent inclusions.

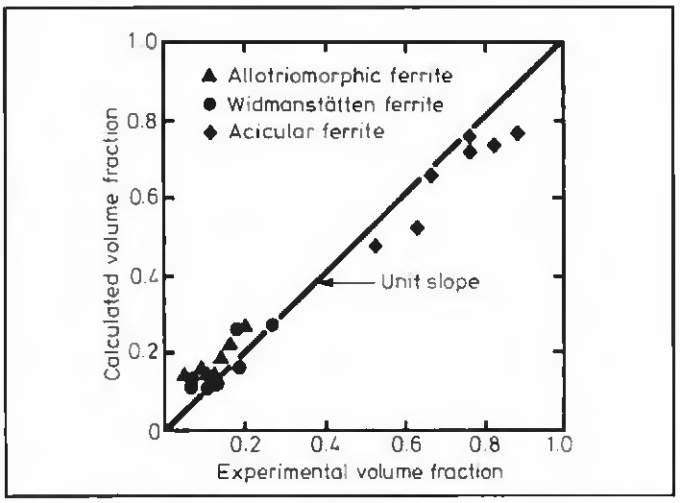

Fig. 8 — An example of the agreement achieved between the measured and calculated weld metal microstructures.

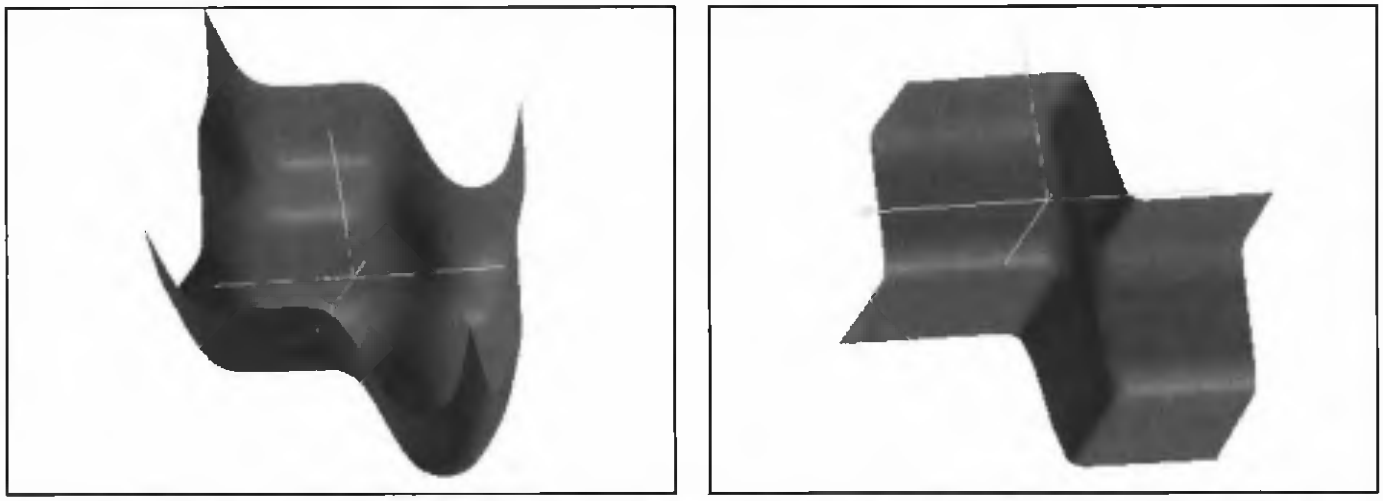

Fig. 9 — Illustration of the complexity of the function (of two inputs) that can be created using a simple neural network with just four hidden units. The two figures are generated for the same mathematical function but different weights.

ρ_D dislocation density, typically 10^{16} m^{-2}

L measure of the ferrite plate size, typically 0.2 μm

Given the microstructure, the yield strength can be estimated from that of the individual phases, either as a rule of mixtures, i.e., $\sigma = \Sigma_i \sigma_i V_i$ where V_i is the fraction of phase i, and $\sigma_i$the corresponding strength. More sophisticated methods for combining the effects of the different phases are also available, but suffice it to say that given the microstructure, it is possible, using well-established strengthening theory, to estimate the weld metal yield strength.

Complex Properties

The fabrication of useful devices and structures is based on more than just the strength. Properties such as fatigue, toughness, stress-corrosion resistance, creep resistance, etc. are routine considerations in the design process (Ref. 13). These properties are "complex" in the sense that they can be measured and used in design but cannot be predicted. There is no theory that has the rigor or sophistication to handle the large number of variables that are known to control such properties.

The conventional way to approach such problems is to apply regression analysis in which experimental data are best-fitted to some function, which is usually linear. The result is an equation in which each of the inputs x_j is multiplied by a weight w_j; the sum of all such products and a constant θ then gives an estimate of the output $y = \Sigma_j w_j x_j + \theta$. This is precisely how the carbon-equivalent equations are derived.

A neural network is a more general method of regression analysis. As before, the input data x_j are multiplied by weights, but the sum of all these products forms the argument of a hyperbolic tangent (Refs. 14, 15). The output y is therefore a nonlinear function of x_j, the function usually chosen being the hyperbolic tangent because of its flexibility. Combining many of these functions increases the available flexibility. A few of the advantages of the network over conventional regression can be listed as follows:

1. There is no need to specify a function to which the data are to be fitted. The function is an outcome of the process of creating a network.

2. The network is able to capture almost arbitrarily nonlinear relationships.

3. With Bayesian methods, it is possible to estimate the uncertainty of extrapolation.

We shall now discuss these last two points in detail.The complexity and flexibility of the relationship that can be cre-

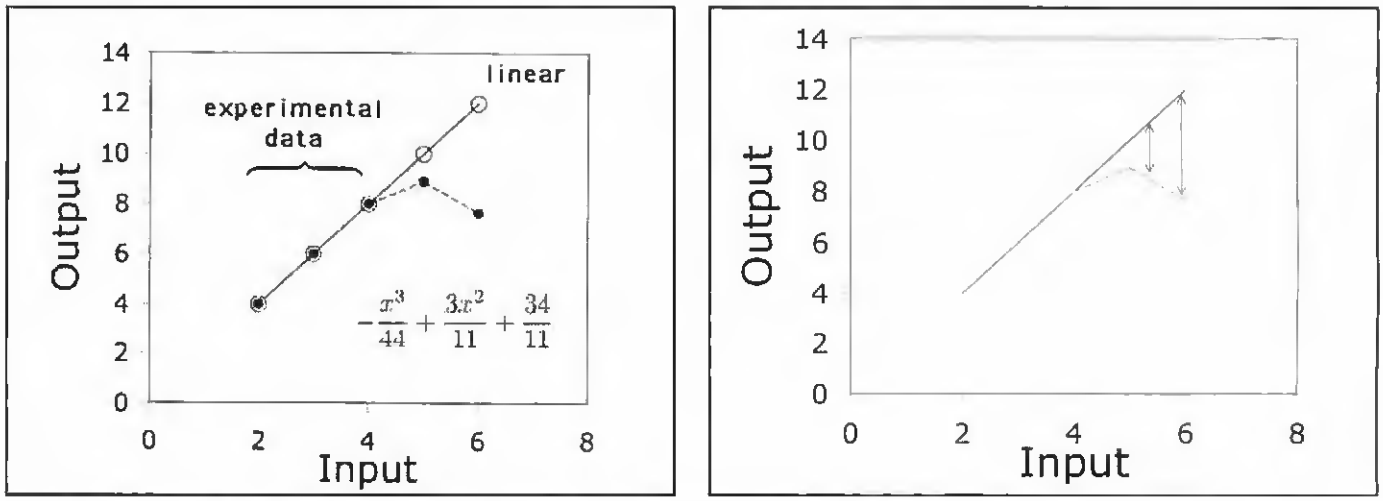

Fig. 10 — Two functions that exactly match the experimental data (2, 4, 6) extrapolate differently.

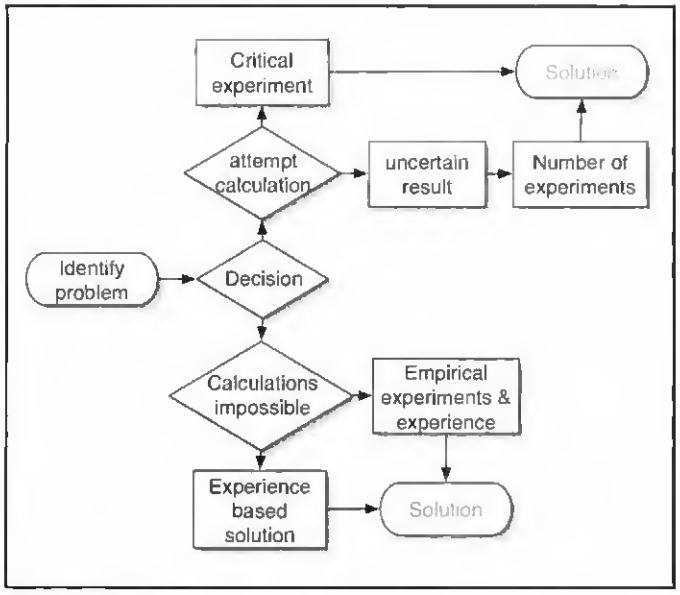

Fig. 11 — Recommended paths in the process of alloy development.

ated is illustrated here (Fig. 9) using just four hyperbolic tangent functions ("hidden units") for two input variables

$$y = tanh\{wx_1 - 2\} + tanh\{x_1^2 - w\} + tanh\{wx_2 + 2\} + tanh\{z_2^2 - w\} + 1 \quad (10)$$

The shape of the surface illustrated changes dramatically as the weights are altered from $w = 3.5$ to $w = 10$. Imagine what can be done using many more hyperbolic tangents, variables, and weights.

The point about extrapolation is illustrated in Fig. 10. The input values 2, 3, and 4 represent experimental data. Both the linear and nonlinear functions exactly represent the experimental data, but make different predictions when it comes to input values 5 and 6, i.e. when the functions are used to extrapolate beyond the experimental data. It is impossible, without physical understanding, to choose between these two.

This could be interpreted as a crisis, but instead, the difference in the predicted values can be taken as an indication of the uncertainty of extrapolation. This uncertainty arises because the functions representing the data extrapolate differently. It is extremely useful to have this indication of uncertainty when dealing with nonlinear functions that are not physically based. MacKay's work has been seminal in expressing neural networks in a Bayesian framework so that the modeling uncertainties become transparent (Ref. 16).

There are now examples where neural networks, in combination with microstructural calculations and experience, have short-circuited the development of welding alloys. A number of these cases are documented in the series of books on the *Mathematical Modelling of Weld Phenomena I–VII*. One desirable feature of the network models is that they are readily updated as more experimental data become available. This is often paraphrased by saying that the models continue to learn and extend their knowledge base.

Proposal for Alloy Development Procedures

Mathematical models of welding will never replace experiments — the problem is too complicated to deal with. There is no doubt, however, that so much tremendous progress has been made that it can justifiably be argued that the process of welding consumable design should begin with calculations in the manner summarized in Fig. 11.

Once the need for the development of a new alloy is identified and design requirements have been formulated, the first step should be an attempt at calculations. There is a plethora of freely accessible software that can be used for this purpose. If a convincing theoretical solution emerges, a critical experiment can be designed in which a consumable is manufactured and tested.

There are circumstances where the calculations will look reasonable but the uncertainties (error bars) associated with the outcomes are large. A series of carefully designed experiments can be implemented to resolve the uncertainties. It would be of long-term benefit to the community if the data associated with these experiments are published so that the models can be modified for greater reliability.

If, at the decision stage (Fig. 11), calculations are impossible because the appropriate models do not exist (for example, creep-fatigue theory), it is justified to conduct empirical experiments based on experience.

It will be fascinating to see how alloy design progresses over the next few years, whether the practitioners are courageous enough to try using models and whether those who develop models have the appreciation necessary to recognize the complexity of welding. The models discussed here are freely available on

http://www.msm.cam.ac.uk/map/map-main.html.

Finally, it should be emphasized that much of this work would not have been possible without the enormous amount of experimental work and contributions to understanding from a large number of people involved in the subject. References to that work are listed in Refs. 1–14. I apologize that it is not possible to present them in this short article.

Acknowledgments

I am immensely grateful to the American Welding Society for the opportunity to present this lecture and to many colleagues in industry and academia who have helped my career in welding metallurgy.

References

1. Grong, Ø. 1997. *Metallurgical Modelling of Welding*, 2nd edition. London: Institute of Materials, pp. 1–602.

2. Easterling, K. E. 1992. *Introduction to the Physical Metallurgy of Welding*, 2nd edition. Butterworths-Heineman.

3. Svensson, L.-E. 1994. *Control of Microstructures and Properties in Steel Arc Welds*. London: CRC Press.

4. Bhadeshia, H. K. D. H., Svensson, L.-E., and Gretoft, B. 1985. *Acta Metallurgica* 33: 1271–1283.

5. Bhadeshia, H. K. D. H. and Svensson, L.-E. 1993. *Mathematical Modelling of Weld Phenomena*. Eds. H. Cerjak and K. E. Easterling. London: Institute of Materials, pp. 109–182.

6. Mundra, K., DebRoy, T., Babu, S. S., David, S. A., and Paul, A. J. 1995. *Modelling of Casting, Welding and Advanced Solidification Processes*, VII. Eds. M. Cross and J. Campbell, TMMMS, pp. 31–38.

7. Weisman, C. ed. 1981. *Welding Handbook*, 7th edition. Miami, Fla.: American Welding Society.

8. Svensson, L.-E, Gretoft, B., and Bhadeshia, H. K. D. H. 1986. *Scandinavian Journal of Metallurgy* 15: 97–103.

9. Bhadeshia, H. K. D. H., Svensson, L.-E., and Gretoft, B. 1986. *Journal of Materials Science* 21: 3947–3951.

10. Bhadeshia, H. K. D. H. 1982. *Metal Science* 16: 159–165.

11. Bhadeshia, H. K. D. H. 1992. *International Trends in Welding Research*. Eds. S. A. David and J. M. Vitek. Materials Park, Ohio: ASM International, pp. 213–222.

12. Bhadeshia, H. K. D. H., and Svensson, L.-E. 1997. *Mathematical Modelling of Weld Phenomena III*. Eds. H. Cerjak and H. K. D. H. Bhadeshia. London: Institute of Materials, pp. 229–284.

13. Bhadeshia, H. K. D. H. 1999. *Trends in Welding Research*. Eds. S. A. David, T. DebRoy, J. A. Johnson, H. B. Smartt, and J. M. Vitek. Materials Park, Ohio: ASM International, pp. 795–804.

14. Bhadeshia, H. K. D. H. 1999. *ISIJ International* 39: 966–979.

15. Bhadeshia, H. K. D. H. 2001. *ISIJ International* 41: 626–640.

16. MacKay, D. J. C. 2003. *Information Theory, Inference and Learning Algorithms*. U.K.: Cambridge University Press.

Preparation of Manuscripts for Submission to the *Welding Journal* Research Supplement

All authors should address themselves to the following questions when writing papers for submission to the Welding Research Supplement:

- Why was the work done?
- What was done?
- What was found?
- What is the significance of your results?
- What are your most important conclusions?

With those questions in mind, most authors can logically organize their material along the following lines, using suitable headings and subheadings to divide the paper.

1) **Abstract.** A concise summary of the major elements of the presentation, not exceeding 200 words, to help the reader decide if the information is for him or her.

2) **Introduction.** A short statement giving relevant background, purpose, and scope to help orient the reader. Do not duplicate the abstract.

3) **Experimental Procedure, Materials, Equipment.**

4) **Results, Discussion.** The facts or data obtained and their evaluation.

5) **Conclusion.** An evaluation and interpretation of your results. Most often, this is what the readers remember.

6) **Acknowledgment, References and Appendix.**

Keep in mind that proper use of terms, abbreviations, and symbols are important considerations in processing a manuscript for publication. For welding terminology, the *Welding Journal* adheres to AWS A3.0:2001, *Standard Welding Terms and Definitions*.

Papers submitted for consideration in the Welding Research Supplement are required to undergo Peer Review before acceptance for publication. Submit an original and one copy (double-spaced, with 1-in. margins on 8 ½ x 11-in. or A4 paper) of the manuscript. A manuscript submission form should accompany the manuscript.

Tables and figures should be separate from the manuscript copy and only high-quality figures will be published. Figures should be original line art or glossy photos. Special instructions are required if figures are submitted by electronic means. To receive complete instructions and the manuscript submission form, please contact the Peer Review Coordinator, Doreen Kubish, at (305) 443-9353, ext. 275; FAX 305-443-7404; or write to the American Welding Society, 550 NW LeJeune Rd., Miami, FL 33126.